

A study around the improvement of electrochemical activity of MnO₂ as cathodic material in alkaline batteries

M. Ghaemi^a, A. Gholami^a, R.B. Moghaddam^{b,*}

^a Department of Chemistry, Science Faculty, Tarbiat Modares University, Tehran, Iran

^b Department of Chemistry, K.N. Toosi University of Technology, 15875-4416 Tehran, Iran

Received 31 May 2007; received in revised form 4 September 2007; accepted 13 October 2007

Available online 22 October 2007

Abstract

An optimized combination of reduction by methane and sulfuric acid digestion was developed to improve the electrochemical activity of manganese dioxide at a battery set. Chemical manganese dioxide, CMD, and electrolytic manganese dioxide, EMD, which have been destroyed after discharge cycling process in potential window of 900–1650 mV versus Hg/HgO, were reduced in a furnace with a flow of methane at 300 and 250 °C correspondingly. Thereafter, the reduced samples, CMDr and EMDr, were digested in a solution of sulfuric acid with optimized concentration and temperature. It was found that digested samples, CMDro and EMDro, typically show more stability in cycling, higher capacity and more reversible redox reaction. Alternatively, we reported about the effect of digestion temperature on electrochemical and structural properties of the samples. Digestion at temperatures 60 and 98 °C in 1.5 M sulfuric acid as superior concentration was preferred after comparative experiments in the range 40–98 °C. The samples which were digested in 60 °C (CMDro1 and EMDro1) showed superior electrochemical activity at the early stages of discharge cycling. By contrast, the samples which were obtained at 98 °C (CMDro2 and EMDro2) showed more stability and were superior to the former samples in final stages of discharge cycling process. Afterward, the electrochemical behavior of the pretreated samples was investigated by means of cyclic voltammetry technique and discharge cumulative capacity profiles. Also X-ray diffraction was employed to verify the responses of voltammetric methods. In XRD patterns, peak at $2\theta = 28.6^\circ$ which is due to β -MnO₂ type was the strongest signal as temperature 98 °C was selected for digestion. After digestion at 60 °C, the characteristic peaks at $2\theta = 38^\circ$ and 42° were amplified which are attributed to formation of γ -MnO₂. Interestingly enough, the results according to the XRD patterns were in good agreement with the electrochemical approaches. © 2007 Elsevier Ltd. All rights reserved.

Keywords: Manganese dioxide; Alkaline battery; Rechargeable battery; Digestion; Modification

1. Introduction

Manganese dioxide is definitely the most widespread electroactive cathode material used in primary batteries. Unique combination of beneficial physicochemical, electrochemical and economic properties of manganese dioxide cells is the most reason for the superiority. In particular, manganese dioxide with suitably high density and purity, as well as adequate electrochemical activity under a range of discharge conditions, can be produced efficiently and relatively inexpensively on a commercial scale [1]. Manganese oxides are known to be active catalysts in several oxidation or reduction reactions and can be used as catalysts for the oxidation of methane and carbon monoxide

[2]. Moreover, the application of manganese oxides as an oxygen storage component (OSC) for a three-way catalyst has been proposed [3]. In all of the applications, the redox properties of manganese oxides play a key role. In a practical application, manganese dioxide can be used as a desirable catalyst for oxidation of methane. The catalytic oxidation of methane over manganese oxide is supposed to proceed through a Mars and van Krevelen mechanism [2]. In principle, manganese oxides may be able to oxidize methane in the absence of gas phase oxygen while oxygen component of manganese dioxide should be consumed during the process. During the reduction of manganese oxide with methane, carbon dioxide and water were the main products [4–6]. The oxidation of manganese oxides is reversible up to Mn₂O₃, re-oxidation to MnO₂ in pure oxygen only proceeds at pressures higher than 3000 bar while the most preferred compound for pursuing the higher electrochemical activity is MnO₂ [7]. However, many attempts have been directed to pro-

* Corresponding author. Tel.: +98 21 2285 35 51; fax: +98 21 2285 36 50.
E-mail address: moghaddam@sina.kntu.ac.ir (R.B. Moghaddam).

duce manganese dioxide with modified pattern for any variable conditions as temperature, pressure, concentration, etc. [8,9]. Therefore, any combination of these variables should lead to deposition of γ - MnO_2 (the preferred structure for electrochemical application) while the variable ranges that produce a superior material are very narrow indeed [10].

The scope of the present work is to develop a modified combination of variables for reduction of inactive manganese oxides by methane followed by oxidation of the reduced compounds by digestion in a solution of sulfuric acid. This method was used for recovery of destroyed cathodic material of a rechargeable alkaline manganese dioxide battery. Also, we have discussed over the role of temperature and concentration of digestion medium and its influences on some defects in manganese dioxide crystalline using potentiometric titration.

2. Experimental

2.1. Reagents

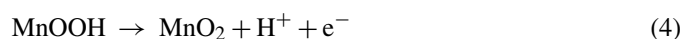
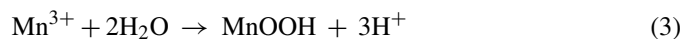
Sulfuric acid, potassium hydroxide, potassium permanganate and sodium pyrophosphate used in this work were Merck products of analytical grade and used as received. Methane was the Iranian Gas Company origin. Doubly distilled water was used throughout the experiment.

2.2. Synthesis of electrolytic manganese dioxide (EMD)

Synthesis was performed at a graphite substrate which has been polished with emery paper prior to use. Electrolyte composition containing MnSO_4 112 g l^{-1} in $0.10 \text{ M H}_2\text{SO}_4$ solution was refluxed in bath temperature of 97 – 98°C and at substrate temperature 135°C for 72 h [9]. Electrolysis was carried out at a rather low current density (5 mA cm^{-2}) to hold a lower value of the anodic over-potential. This is to avoid defective EMD structures caused by rapid growth at the electrode surface. The precipitates obtained were removed mechanically from the anode and washed several times with distilled water. The products were then ground with a mortar and pestle and neutralized using 10% ammonia solution. Subsequently, the samples were dried at 80°C overnight. The overall reaction for deposition of MnO_2 is given by:



Paul and Cartwright [11] proposed a model for the electrochemical oxidation of Mn^{2+} , i.e.,



The product was then filtered through a $100 \mu\text{m}$ mesh sieve in order to be used in rechargeable alkaline manganese dioxide (RAM) batteries.

2.3. Materials preparation and nomination

Two different kinds of manganese dioxide were used within this study. Chemical manganese dioxide (CMD) was Merck Sample and electrolytic manganese dioxide (EMD) which was synthesized as previously stated. EMDd is obtained when EMD in rechargeable alkaline MnO_2 – Zn battery is charged and discharged after 70 consecutive cycles. Manganese dioxide, graphite and acetylene black which form the cathode of the battery, were washed thoroughly with distilled water till the washing solution became neutral. Thereafter, the sample was left in quartz furnace. During the reduction of manganese oxide with methane, carbon dioxide and water were the main byproducts. Reduction was carried out at 300°C for CMD and 250°C for EMDd with methane (100 ml/min) for 12 h . Finally the samples were cooled down. Reduced CMD and EMDd are nominated as CMDr and EMDr, respectively. Thus, the reduced MnO_2 digests into H_2SO_4 solutions of different concentrations (up to 3 M) at various temperatures (up to 98°C). For digestion, 0.5 g of CMDr or EMDr sample was suspended in 50 cm^3 of sulfuric acid of a given concentration. Then, suspension was heated in medium temperatures 40 , 60 , 70 , 80 , 98°C for 24 h . After the time, the suspension was filtered and washed with distilled water. The resulting solids were dried in air. The samples which were produced were typically nominated MDro. Generally, after reduction by methane followed by digestion in sulfuric acid in 60 and 98°C , the products were named as MDro1 and MDro2, respectively.

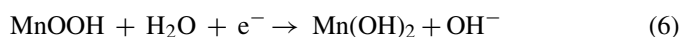
2.4. Instrumentation

Electrochemical studies were carried out in a conventional three electrode cell powered by a model 273A EG&G potentiostat/galvanostat. The system was run by a PC through M270 commercial software. The working electrode potential monitored against an Hg/HgO standard reference electrode and a Pt plate formed the counter electrode. A model Philips Xpert diffractometer and $\text{Cu K}\alpha$ radiation ($\lambda = 0.15418 \text{ nm}$) were employed to record X-ray diffraction patterns. Charging of the samples was carried out at constant current 10 mA g^{-1} .

3. Results and discussion

3.1. Characterization of CMD and EMD

Fig. 1 presents a typical cyclic voltammogram of CMD in 9 M KOH at potential sweep rate of 0.25 mV s^{-1} in the range -800 – 400 mV versus Hg/HgO . Two irreversible cathodic peaks around -150 and -350 mV are observed which can be assigned to reduction processes as following [12–14]:



Formation of Mn(OH)_2 is believed to be irreversible and restricts the reverse reaction in the anodic direction. Continuous reduction of unreduced manganese dioxides in the reverse

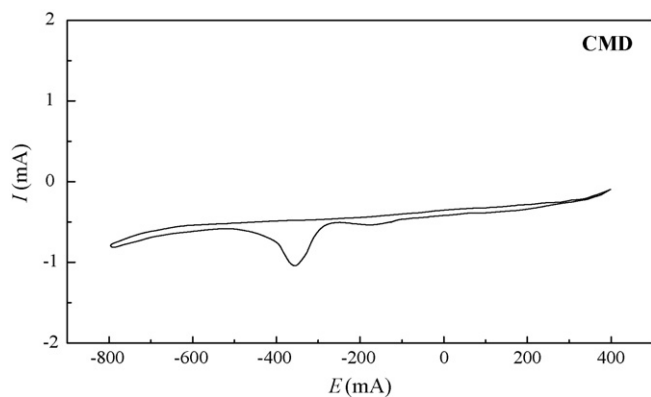


Fig. 1. Cyclic voltammogram of CMD in 9M KOH in the potential range -800 – 400 mV at potential sweep rate of 0.25 mV s^{-1} .

direction results in the negative current of voltammogram in the anodic sweep leading one to conclude that CMD is composed of almost inactive manganese dioxides. Fig. 2 presents discharge cumulative capacity of CMD as a function of cycle number during 15 consecutive cycles in the potential range of 900 – 1650 mV versus Hg/HgO at constant current 30 mA g^{-1} . As can be seen, the values of cumulative capacity in all stages of discharge are not desirable. It can be predicted that α - MnO_2 and β - MnO_2 in crystalline structure of CMD are the main features. These types are structural compositions of manganese dioxide with relatively low electrochemical activity.

Fig. 3 presents CVs of EMD before and after undergone 70 consecutive battery cycles within the same captions as Fig. 1. The voltammogram obtained under these conditions is identical to that given in the literature [15]. With taking into account that the broad cathodic shape around -40 mV can be composed of two overlapping peaks concerning the reduction of manganese dioxide, it would be interesting to reveal that the surface and inside manganese dioxides have been reduced in different potential values. Over-potential for the reduction of inside manganese dioxides is supposed to be slightly more than that of on the surface. Alternatively, two anodic peaks in the potentials -220 and 220 mV are probably assigned to the oxidation of the surface

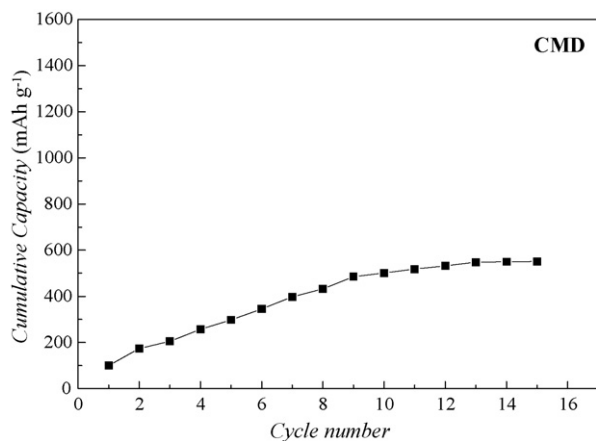


Fig. 2. Discharge cumulative capacity of battery based on CMD as a function of cycle number in the range 900 – 1650 mV recorded at initial 15 cycles and at constant current 30 mA g^{-1} .

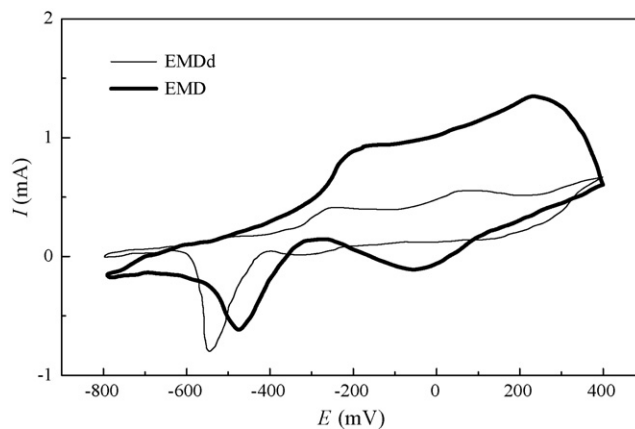


Fig. 3. Typical CVs of EMD and EMDd in 9M KOH in the range -800 – 400 mV and at potential sweep rate of 0.25 mV s^{-1} .

and inside MnOOH . This further amplifies the argument that the kinetics of $\text{Mn}(\text{OH})_2$ oxidation is poor and can reasonably prevent the reversibility of the redox reactions. Additionally, the plot of EMDd depicts that the cycling of EMD dramatically decreases the capacity of the electro-active materials since current is proportional to capacity.

Fig. 4 shows discharge cumulative capacity of test battery containing EMD within the 70 consecutive cycles at constant current of 30 mA g^{-1} . The plot has been recorded at cycles 10, 20, 30, 40, 50, 60 and 70 which after any 10 cycles, cathodic materials were extracted and washed with water and then dried in air in order to fabricate a new battery set. Accordingly, discharge cumulative capacity improved after the washing and drying operation. This pathway is observed till the cycle 30. After that, capacity greatly diminishes since the cathodic materials have been altered to the less active compounds. Formation of undesirable types of manganese oxides can be responsible for lowering of the capacity since these compounds are not properly electro-active [9].

The basis for the currently accepted discharge mechanism ($\text{Mn}(\text{IV}) \rightarrow \text{Mn}(\text{III})$) was proposed by Kozawa et al. [16–18], and is constructed on proton and electron insertion into the manganese dioxide structure. Typically, the cathode in an alkaline

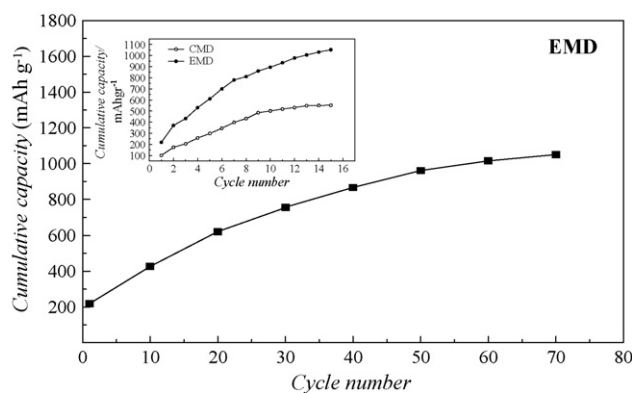


Fig. 4. Discharge cumulative capacity of battery based on EMD as a function of cycle number in the range 900 – 1650 mV in 70 consecutive cycles recorded after any 10 cycles; comparison between CMD and EMD at initial 15 cycles (inset).

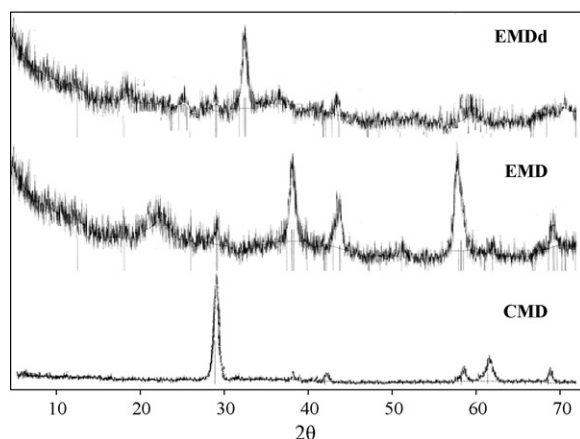
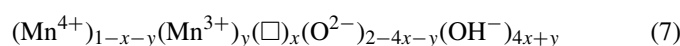


Fig. 5. X-ray diffraction patterns of CMD, EMD and EMDd.

Zn/MnO₂ cell essentially consists of an intimate mixture of electrolytic manganese dioxide (EMD) and a small proportion of graphite wetted with electrolyte. An electron from the external circuit passes through the graphite into the manganese dioxide structure where it reduces a Mn(IV) to Mn(III). For charge compensation, a water molecule on the manganese dioxide surface dissociates into a proton, which is inserted into the structure, and an OH⁻ ion, which remains in the electrolyte. Additional capacity (other than that on the surface) can be extracted from the manganese dioxide by the inserted protons and electrons diffusing away from the surface into the bulk of the solid. In the light of the previous study [1], it can be stated that within the hexagonal close-packed framework of oxide anions, a fraction of Mn(IV) ions have been replaced by Mn(III) (*y*), and that a fraction of Mn(IV) ions are absent altogether (*x*). The positive charge deficiency is compensated by an appropriate number of protons located on adjacent oxide ions [1]:



where \square represents a cation vacancy. Typical ranges for *x* and *y* are 0.06–0.08 and 0.04–0.12, respectively. It is these protons that constitute structural water within γ -MnO₂.

To guarantee the accuracy of the voltammetric studies, X-ray diffraction patterns, Fig. 5, was employed. XRD plots of CMD are composed of a strong peak in $2\theta = 28.6^\circ$ attributed to α -MnO₂ and/or β -MnO₂, and two weak peaks at $2\theta = 38^\circ$ and 42° which are assigned to the presence of γ -MnO₂ [19,20]. Apparently, weakness of the characteristic peaks around $2\theta = 38^\circ$ and 42° in this pattern, is due to the existing of the low concentration of γ -MnO₂. Consequently as stated before, α -MnO₂ and β -MnO₂ seem to be the main types in a CMD sample. Strong peaks around $2\theta = 38^\circ$ and 42° and a weak peak around $2\theta = 28.6^\circ$ are the main features in XRD pattern of EMD. This clearly shows γ -MnO₂ is the dominant type in EMD. Appearance of a strong signal at around $2\theta = 33^\circ$ in XRD of EMDd is indexed to the formation of Mn₂O₃ [21]. On the basis of the results, it can be assumed that pyrolusite is the main type forming CMD while EMD is mostly composed of ramsdellite.

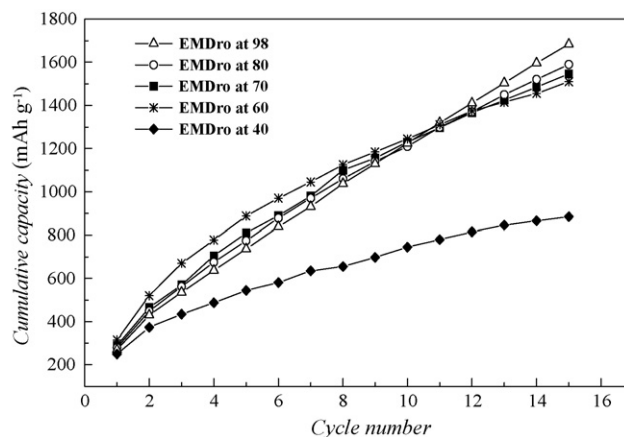


Fig. 6. Discharge cumulative capacity of EMDro as a function of cycle number at various medium temperatures; the other captions are the same as Fig. 4.

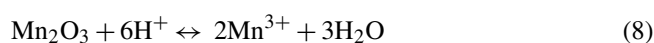
3.2. Modification treatments

Initially, CMD and EMDd were reduced in a flow of methane (100 ml min⁻¹) at temperatures 300 and 250 °C correspondingly. Subsequently, the reduced samples were digested in a solution of sulfuric acid in optimized medium temperature and concentration. In order to determine the optimized temperatures for digestion of CMDr and EMDr, a comparison was performed in the range 40–98 °C in a 1.5 M medium of sulfuric acid. Fig. 6 shows the cumulative capacity of EMDro as a function of cycle number at constant current 30 mA g⁻¹ recorded in various medium temperatures. According to the measurements, it is originated in that digestion of samples at higher temperatures results in formation of more stable structural types of manganese dioxide. After digestion at 60 °C, the capacity slowly decreases within the seven initial cycles. At the second half of the measurement, faster decrease of the capacity indicates that EMDro1 is relatively unstable. After digestion at 98 °C, the product (EMDro2) is more stable as its cumulative capacity is superior to EMDro1 in final cycles. This approach is in agreement with the Ohzuku et al. report [22].

Fig. 7 presents comparative discharge cumulative capacity of EMDro after digestion at various medium concentrations within the 15 consecutive cycles. Meaningful decrease of capacity is considered both in higher and lower sulfuric acid concentration than 1.5 M. Increment of acid concentration leads to expected increase in the oxidation rate. As a result of this, necessary time for oxidizing of Mn(III) could not be provided with take it into consideration that the rate of Mn(III) oxidation is believed to be low [15]. Simultaneously, an electron transfer between two neighbor Mn(III) is occurred.

Without going into details, the mechanism of the interaction can be proposed via a dissolution process followed by a disproportionation–precipitation step [1,23]:

- Dissolution:



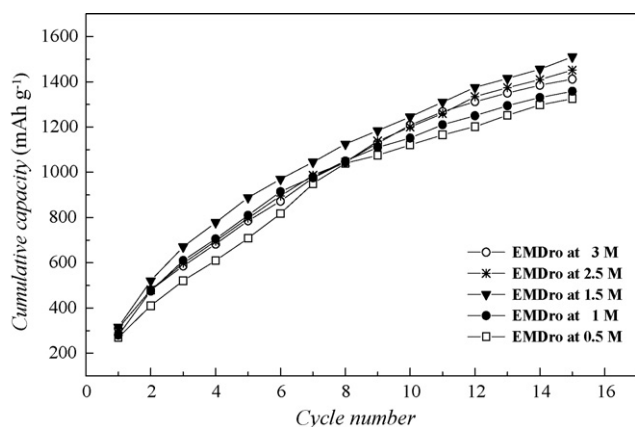


Fig. 7. Discharge cumulative capacity of EMDro as a function of cycle number at various medium concentrations within the 15 consecutive cycles in the range 900–1650 mV and at constant current 30 mA g^{-1} .

- Disproportionation–precipitation:



- Overall reaction:



At the final stages of this interaction, formed Mn(II) leaves the crystalline structure and accordingly, a cation vacancy left-overs. Therefore, the amount of vacancies increases rapidly as acid concentration is raised. Generally, at discharge cycle in alkaline cells, an electron can diffuse via the conductor towards the surface manganese dioxides. Reduction of inside manganese dioxides is carried out through the diffusion of a proton into the structure [23]. Increment of cation vacancies leads to provide more available sites for proton substitution and this can probably increase the rate of proton diffusion. By contrast, decrease of manganese dioxide concentration of structure as a result of overproduction of cation vacancy, may dramatically decrease the capacity values. Consequently, at higher concentration of sulfuric acid than 1.5 M, the capacity diminishes gradually.

Potentiometric titration was performed to calculate the cation vacancy fraction as well as Mn(III) fraction (y) in order to shed more light on prevailing mechanism. The method of calculation has been formerly explained by Walanda et al. [1]. According to the literature, the fraction of Mn(III) ions in the MnO_2 structure (y) can be quite readily determined by potentiometric titration. Table 1 shows the quantity of Mn(III) fraction in MnO_2 structure in relation to medium concentration. The Ruetschi cation

Table 1
Mn(III) fraction of EMDro as a function of medium concentration at temperature 60°C

Sample	H_2SO_4 Conc. (M)	Temperature ($^\circ\text{C}$)	Mn(III) fraction
EMDro	0.5	60	0.12
EMDro	1	60	0.1
EMDro	1.5	60	0.09
EMDro	2.5	60	0.07
EMDro	3	60	0.04

Table 2

Cation vacancy fraction of EMDro as a function of medium concentration at temperature 60°C

Sample	H_2SO_4 Conc. (M)	Temperature ($^\circ\text{C}$)	Cation vacancy
EMDro	0.5	60	0.05
EMDro	1	60	0.1
EMDro	1.5	60	0.13
EMDro	2.5	60	0.18
EMDro	3	60	0.19

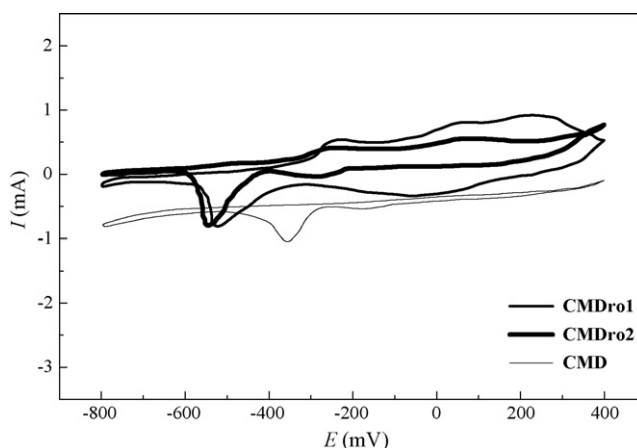


Fig. 8. Cyclic voltammograms of CMD, CMDro1 and CMDro2 in the potential window of -800 – 400 mV in 9M KOH; potential sweep rate was 0.25 mV s^{-1} .

vacancy fraction is also an indicator of the level of structural defects within γ - MnO_2 crystalline [24]. Table 2 shows cation vacancy as a function of medium concentration at temperature 60°C .

Fig. 8 presents cyclic voltammograms of CMD, CMDro1 and CMDro2 in the potential window of -800 – 400 versus Hg/HgO in 9M KOH and Fig. 9 presents CVs of EMDd, EMDro1 and EMDro2. After thermal treatment on the destroyed cathodic materials, typical mechanism of redox reactions of EMD seems to be unchanged since the overall pattern of voltammograms remains identical. In contrast, irreversibility of CMD is

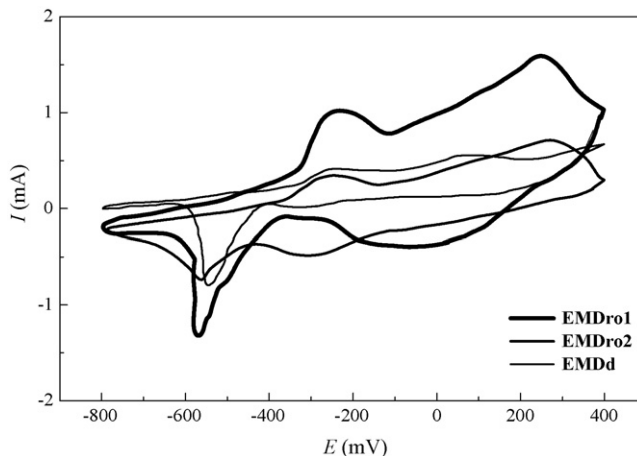


Fig. 9. Cyclic voltammograms of EMDd, EMDro1 and EMDro2 in the range -800 – 400 mV in 9M KOH at potential sweep rate of 0.25 mV s^{-1} .

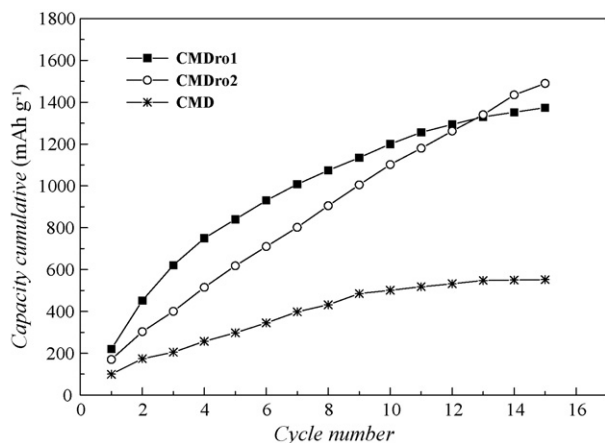


Fig. 10. Comparative discharge cumulative capacity of CMD, CMDro1 and CMDro2 as a function of cycle number in the range 900–1650 mV recorded at first 15 cycles and at constant current 30 mA g⁻¹.

believed to be changed to a more reversible redox system. Interestingly, the treatment has definitely recovered the destroyed manganese dioxide both in CMD and EMD. Moreover, the current densities have been dramatically increased. Without much speculation, it is obviously unveiled that reduction by methane followed by digestion in a solution of sulfuric acid has expanded the integrated region of faradic and non-faradic charge transfer.

Cumulative capacities of CMD, CMDro1 and CMDro2 have been compared in Fig. 10. As previously demonstrated and on the basis of this plot, it is resulted that the capacities of CMDro1 and CMDro2 are dramatically enhanced compared to CMD at all discharge steps. On the other hand, capacity of CMDro1, which has been obtained of digestion in 60 °C, is superior to CMDro2 in the early stages of discharge process. By contrast, its capacity decays more rapidly than CMDro2 as discharge proceeds. Similarly, these results are repeated typically in EMDs, Fig. 11, accompanied by the fact that the capacity of EMDro is quantitatively larger in comparison with CMDro. These obser-

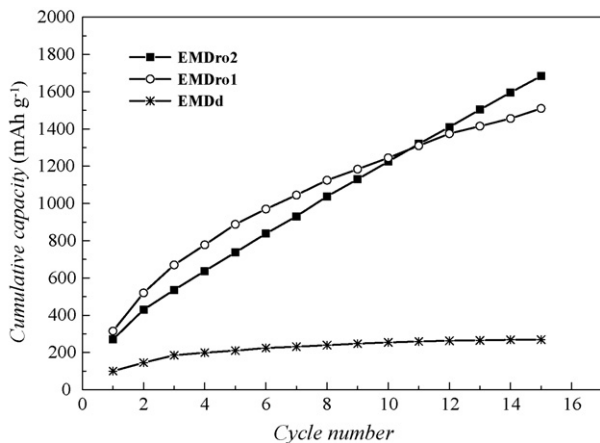


Fig. 11. Comparative discharge cumulative capacity of EMD, EMDro1 and EMDro2 as a function of cycle number in the range 900–1650 mV recorded at first 15 cycles and at constant current 30 mA g⁻¹.

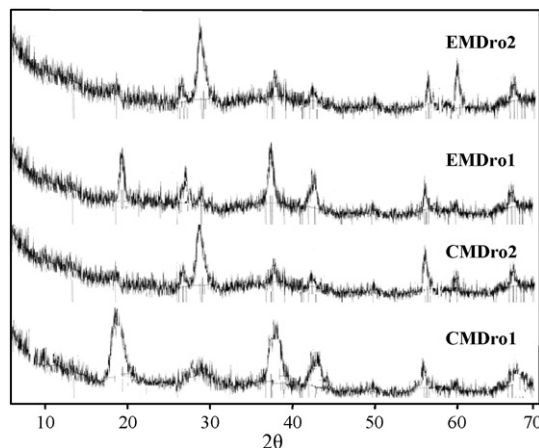


Fig. 12. X-ray diffraction patterns of CMDro1, CMDro2, EMDro1 and EMDro2.

vations evidently show that the sample which has been digested at temperature 60 °C shows better electrochemical activity and less stability than the sample which has been digested in 98 °C.

XRD plots of CMDro1, EMDro1, CMDro2 and EMDro2, Fig. 12, further verify the accuracy of the results. At Fig. 12, signals around $2\theta = 38^\circ$, 42° are stronger in CMDro1 and EMDro1 in comparison with the other samples. This obviously shows that γ -MnO₂ is dominant crystalline type as digestion is performed in 60 °C. In contrast, a peak in $2\theta = 28.6^\circ$, which is attributed to β -MnO₂, is found in XRD pattern of CMDro2 and EMDro2 [1,21].

Fig. 13 compares the efficiency of the treatment on CMD and EMDd within 15 consecutive cycles. The records indicate that while the recovery process was efficient for both CMD and EMDd, there was a stronger impact on EMDd than on CMD. This can be assigned to different structure of the destroyed samples and/or existing of more inactive manganese oxides in destroyed CMD crystalline than in EMDd.

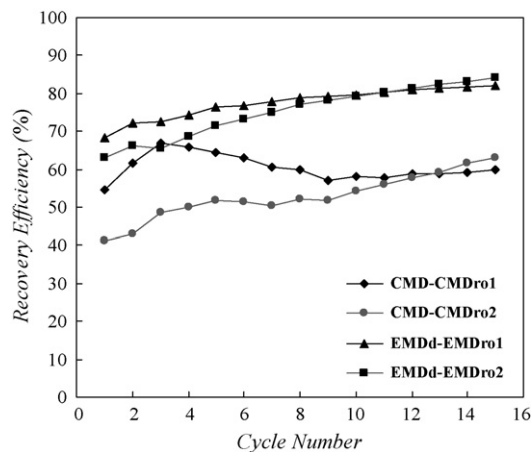


Fig. 13. Efficiency of the recovery process (reduction in an atmosphere of methane followed by digestion in sulfuric acid) for both CMD and EMDd within 15 consecutive cycles.

4. Conclusion

This work presents a coupled method in order to recover less active manganese oxides which are formed after potential cycling. A flow of methane was used for reduction of CMD and EMD at temperatures 300 and 250 °C, respectively followed by an acid digestion for recovery of destroyed samples. Optimum concentration of 1.5 M was found by means of comparative potentiometric titration experiment. Also, digestion was carried out at various medium temperatures to find the optimized temperature. It was found that at 60 °C the most favorable type γ -MnO₂ and at higher temperatures up to 98 °C more stable type β -MnO₂ are formed. At the early stages of discharge cycling process, CMDro1 and EMDro1 show more capacity rather than CMDro2 and EMDro2, respectively. By contrast, with taking into account that samples obtained at higher temperature are more stable, at final stages of discharge, CMDro2 and EMDro2 are superior to CMDro1 and EMDro1 correspondingly. These results were investigated by means of X-ray diffraction profiles and the accuracy of them was verified. Moreover, efficiency of the recovery process was presented which the results clearly showed that the treatment was sufficient for both CMD and EMDd.

Acknowledgements

Financial support of this work by Tarbiat Modares University Research Council is gratefully acknowledged. The authors extend gratitude to Mr. Davoud Moghaddam for his useful comments.

References

- [1] D.K. Walanda, G.A. Lawrance, S.W. Donne, *J. Power Sources* 139 (2005) 325.
- [2] E.R. Stobbe, B.A. de Boer, J.W. Geus, *Catal. Today* 47 (1999) 161.
- [3] Y.F. Chang, J.G. McCarty, *Catal. Today* 30 (1996) 163.
- [4] R. Burri, A. Weber, *J. Power Sources* 57 (1995) 31.
- [5] M. Barak (Ed.), *Electro Chemical Power Sources*, Peter Pregrinus, London, 1980.
- [6] K.V. Kordesch, N.W. Bacher, *J. Power Sources* 51 (1994) 61.
- [7] D. Van de Kleut, PhD Thesis, Utrecht University, 1994.
- [8] M. Ghaemi, L. Binder, *J. Power Sources* 111 (2002) 248.
- [9] M. Ghaemi, R.K. Ghavami, L. Khosravi-Fard, M.Z. Kassaei, *J. Power Sources* 125 (2004) 256.
- [10] R.P. Williams, PhD Thesis, University of Newcastle, 1996.
- [11] R.L. Paul, A. Cartwright, *J. Electroanal. Chem.* 201 (2003) 123.
- [12] D.A. Fieldler, J.O. Besenhard, M.H. Fooker, *J. Power Sources* 69 (1997) 157.
- [13] J. McBreen, *J. Power Sources* 5 (1975) 525.
- [14] J. McBreen, *Electrochim. Acta* 20 (1975) 221.
- [15] M. Ghaemi, L. Khosravi-Fard, J. Neshati, *J. Power Sources* 141 (2005) 340.
- [16] A. Kozawa, J.F. Yeager, *J. Electrochem. Soc.* 112 (1965) 959.
- [17] A. Kozawa, T. Kalnoki-Kis, J.F. Yeager, *J. Electrochem. Soc.* 113 (1966) 405.
- [18] A. Kozawa, J.F. Yeager, *J. Electrochem. Soc.* 115 (1968) 1003.
- [19] X.G. Zhang, C.M. Shen, H.L. Li, *Mater. Res. Bull.* 36 (2001) 541.
- [20] L.I. Hill, A. Verbaere, D. Guyomard, *J. Power Sources* 119–121 (2003) 226.
- [21] D.A.J. Swinkels, K.E. Anthony, P.M. Fredericks, P.R. Osborn, *J. Electroanal. Chem.* 168 (1984) 433.
- [22] T. Ohzuku, H. Higashimura, T. Hirai, *Electrochim. Acta* 29 (1984) 779.
- [23] J.Y. Welsh, *Electrochem. Tech.* 5 (1967) 504.
- [24] P. Ruetschi, *J. Electrochem. Soc.* 131 (1984) 2737.